T.R.
GEBZE TECHNICAL UNIVERSITY
GRADUATE SCHOOL

EFFECT OF POST PROCESSING HEAT TREATMENT ON THE MICROSTRUCTURE AND HIGH TEMPERATURE MECHANICAL PROPERTIES OF ADDITIVELY MANUFACTURED INCONEL 718 SUPERALLOY

MERVE CANBOLAT

A THESIS OF MASTEROF SCIENCE
DEPARTMENT OF MATERIALS SCIENCE AND ENGINEERING

ADVISOR: ASSOC.PROF.DR. NESLİHAN TAMSÜ SELLİ
Co-ADVISOR: DR. HÜSEYİN AYDIN

OCTOBER 2024

T.R.

GEBZE TECHNICAL UNIVERSITY

GRADUATE SCHOOL

EFFECT OF POST PROCESSING HEAT TREATMENT ON THE MICROSTRUCTURE AND HIGH TEMPERATURE MECHANICAL PROPERTIES OF ADDITIVELY MANUFACTURED INCONEL 718 SUPERALLOY

MERVE CANBOLAT

A THESIS OF MASTER OF SCIENCE

DEPARTMENT OF MATERIALS SCIENCE AND ENGINEERING

ADVISOR: DOÇ. DR. NESLİHAN TAMSÜ SELLİ

Co-ADVISOR: DR. HÜSEYİN AYDIN

OCTOBER 2024

T.C.
GEBZE TEKNİK ÜNİVERSİTESİ
LİSANSÜSTÜ EĞİTİM ENSTİTÜSÜ

EKLEMELİ İMALAT İLE ÜRETİLEN INCONEL 718 SÜPERALAŞIMINA ISIL İŞLEMİN MİKROYAPI VE YÜKSEK SICAKLIK MEKANİK ÖZELLİKLERİ ÜZERİNE ETKİSİ

MERVE CANBOLAT

YÜKSEK LİSANS TEZİ
MALZEME BİLİMİ VE MÜHENDİSLİĞİ
ANABİLİM DALI

DANIŞMAN: DOÇ. DR. NESLİHAN TAMSÜ SELLİ
2. DANIŞMAN: DR. HÜSEYİN AYDIN

EKİM 2024

MASTER of SCIENCE JURY APPROVAL FORM

A thesis submitted by Merve CANBOLAT, defended on 16/10/2024 before the jury formed with the 04/07/2024 date and 2024/34 numbered decision of the GTU Graduate Administration Board, has been accepted as a MASTER of SCIENCE thesis in the Department of Material Science and Engineering.

JURY

MEMBER
(THESIS ADVISOR) : Assoc. Prof. Neslihan TAMSÜ SELLİ

MEMBER : Assoc. Prof. Kerem Özgür GÜNDÜZ

MEMBER : Assoc. Prof. Betül YILDIZ

APPROVAL

Gebze Technical University Graduate Administration Board
……/……/…….. date and …..…./…….. numbered decision.

SIGNATURE/SEAL

ABSTRACT

Additive manufacturing technology provides advantages due to its ability complex shapes with high dimensional precision. The as-manufactured SLM part's microstructural heterogeneity inevitably results in mechanical heterogeneity and it is necessary post processing heat treatments in order to create homogenous microstructures and desired phases. IN 718 is a nickel based superalloy with γ matrix and γ'-Ni3Al, γ''-Ni3Nb, δ-Ni3Nb and laves-(Ni,Fe,Cr)2(Nb,Mo,Ti) phases. γ″ provides a significant role in high temperature strengthening of this alloy.

Melt pool structure is a typical microstructure observed in additively produced IN718 superalloys. Since the melt pools are the reason of microstructural heterogeneity in as-built SLM parts, it is necessary to perform post-process heat treatments in order to create more homogenous microstructures. Therefore, an attempt was made to achieve more homogenous and solid microstructure via post process heat treatments in this study. Conventional heat treatment procedures were applied and compared with modified heat treatment recipes.

Keywords: Superalloy, Additive Manufacturing, Heat Treatment

ÖZET

Eklemeli imalat teknolojisi, yüksek boyutsal hassasiyete sahip karmaşık şekiller oluşturma kabiliyeti nedeniyle avantajlar sağlamaktadır. Üretilen SLM parçasının mikroyapısal heterojenliği kaçınılmaz olarak mekanik heterojenliğe neden olur ve homojen mikroyapılar ve istenen fazlar oluşturmak için işlem sonrası ısıl işlemler gereklidir. IN718, γ matris ve γ'-Ni3Al, γ''-Ni3Nb, δ-Ni3Nb ve laves-(Ni,Fe,Cr)2(Nb,Mo,Ti) fazlarına sahip nikel bazlı bir süper alaşımdır. γ″ bu alaşımın yüksek sıcaklıkta güçlendirilmesinde önemli bir rol oynar.

Eriyik havuzu yapısı, katkılı olarak üretilen IN718 süper alaşımlarında gözlemlenen tipik bir mikroyapıdır. Eriyik havuzları, üretilmiş SLM parçalarında mikroyapısal heterojenliğin nedeni olduğundan, daha homojen mikroyapılar oluşturmak için işlem sonrası ısıl işlemlerin yapılması gerekir. Bu nedenle, bu çalışmada işlem sonrası ısıl işlemlerle daha homojen ve katı bir mikroyapı elde edilmeye çalışılmıştır. Geleneksel ısıl işlem prosedürleri uygulanmış ve modifiye edilmiş ısıl işlem reçeteleri ile karşılaştırılmıştır.

Anahtar Kelimeler: Süperalaşım, Eklemeli İmalat, Isıl İşlem

ACKNOWLEDGEMENTS

I would like to express my gratitude to my supervisor Doç. Dr. Neslihan TAMSÜ SELLİ for her guidance, support, constructive feedback, endless tolerances, and patience during this thesis.
I would like to express my gratitude to my co-supervisor Dr. Hüseyin AYDIN for his permanent encouragement, wise suggestions, supervision, and guidance from the beginning to the end of this thesis. He always shared his knowledge and experiences with me.
I am deeply grateful to Burak Horasan for his permanent encouragement, help, support and all efforts.
I am grateful to Ph.D. Deniz Sultan AYDIN and Ph.D. Aylin ŞAHİN KAHRAMAN for their help in my SEM and EDS analyses. I would like to express my sincere thanks to Aygün Güngör and İbrahim KÜÇÜKOGUL for their help in mechanical tests. I am grateful to my friends Sena TURAN and Müge AKDEMİR for their friendship.
I am also grateful to my friend Muhammet BOZ for his friendship and support.
Finally, I owe gratefulness to my mother Hatice Sarıoğlu, to my sister Melike CANBOLAT YALÇIN, to my brother Emre CANBOLAT for their endless love, support, encouragement, patience and the opportunities during this study as in the entire of my lifetime.
This thesis was part of “3219504 UP26-SAYEM Eklemeli İmalata Yönelik Yerli ve Özgün Tasarım, Malzeme, Üretim ve Tezgah Teknolojilerinin Geliştirilmesi Platformu” project of TÜBİTAK Metallic Materials Technoloies Research Group which is supported by “SENTES1” company.

TABLE OF CONTENTS

LIST OF SYMBOLS AND ABBREVIATIONS

Hz	: Hertz
F	: Force
km	: Kilometer
H	: Magnetic field vector
sn	: Second
γ'	: Gamma Prime
γ''	: Gamma Double Prime
δ	: Delta
$\dot{\varepsilon}$	: Strain Rate
XRD	: X-Ray Diffraction
SEM	: Scanning Electron Microscope

LIST OF FIGURES

LIST OF TABLES

1. INTRODUCTION

Superalloys are a class of alloys specifically engineered for applications that demand exceptional performance at high temperatures and resistance to oxidation. These alloys are primarily composed of Group VIIIB elements such as iron (Fe), nickel (Ni), and cobalt (Co).

Inconel 718 is a nickel-based superalloy developed by the International Nickel Corporation in the 1950s. It remains widely used across various industries, including aerospace, energy, petrochemicals, and maritime, due to its exceptional mechanical properties and resistance to high temperatures and corrosion. Inconel 718 has γ' (Ni3 (Al, Ti)), γ" (Ni3 Nb) and δ precipitate phases on the γ matrix. Thanks to these phases in its structure, it is used in applications such as high temperature, oxidation, etc. Among these phases, it is the Niobium-rich semi-stable γ" precipitate phase in the BCT (body-centered tetragonal) structure that provides the main strength. In heat treatment processes, this phase is precipitated on the matrix to increase strength and oxidation resistance at high temperatures.

Layer by layer, materials are added to an object during the process of additive manufacturing. Additive manufacturing creates things from the ground up as opposed to traditional manufacturing techniques, which frequently entail removing material from a solid block. Complex geometries and unique shapes can be created thanks to this cutting-edge production process.

1.1. Purpose of Thesis

In this study, the microstructural and high temperature mechanical behavior of additively manufactured Inconel 718 superalloy is examined. To achieve this as-built samples, conventional heat treatment, and modified heat treatment designs were employed to investigate the effects on the material's microstructural development. Additionally, the impact of these microstructural changes on high-temperature tensile and creep properties is also analyzed. The heat treatment design carry out to see the effect of the formation of γ’ ($Ni_3(Ti,Al)$), γ’’ (Ni_3Nb) phases in terms of microstructural and mechanical properties by applying solution heat treatment below

and above the dissolution temperature of the Laves ((Ni, Fe, $Cr)_2$ (Nb, Mo and Ti)) phase.

2. LITERATURE REVIEW

2.1. Additive Manufacturing

Additive manufacturing (AM), sometimes referred to as rapid prototyping, is the method of combining materials from 3D CAD model data to create products. Manufacturing more complicated, functional components that require less energy and can be produced faster than with traditional manufacturing methods is a rapidly expanding industry sector. This method eliminates the need for final assembly or machining by manufacturing the components in a layer-by-layer basis **[1]**.

The ability to fabricate incredibly complex geometric structures in a single manufacturing stage thereby reducing the number of assembly operations is the main advantage of additive manufacturing. Additionally, manufacturers are now able to produce all components, like nuts and screws, with incredibly tight tolerances because to the application of AM technology. As a result, Additive Manufacturing (AM) technology enhances product quality and increases the lifespan of components by minimizing defects. In contrast, traditional manufacturing techniques involve multiple stages to create complex parts. Another significant benefit of the AM process is the flexibility it provides in design . Changes can be made much faster in the production of products manufactured using CAD software. This means that instead of changing the production equipment, only a file design needs to be changed **[1]**.

2.1.1. Selective Laser Melting

Selective laser melting (SLM) is an additive manufacturing method that enables the production of complex metal components directly from 3D-CAD models, achieving nearly complete density and high dimensional precision in a single process. The method works on the direct layer-by-layer construction of the components by the carefully regulated melting of metal powders using a concentrated laser beam. According to the cross-sectional shape of the component to be manufactured, metal powders are evenly distributed on a platform at a specific layer thickness during the SLM process. Subsequently, the particles are melted using lasers and subsequently solidified to create the layer. A new layer of powder is applied to the platform after it

has been moved down to layer thickness. The portion is taken off the platform after these cycles are repeated until it is finished as desired. The process parameters such as beginning powder composition, scanning method, laser power,layer thickness, etc. have a significant impact on the qualities of the printed objects. Figure 2. provides a schematic representation of the SLM technology **[1]**.

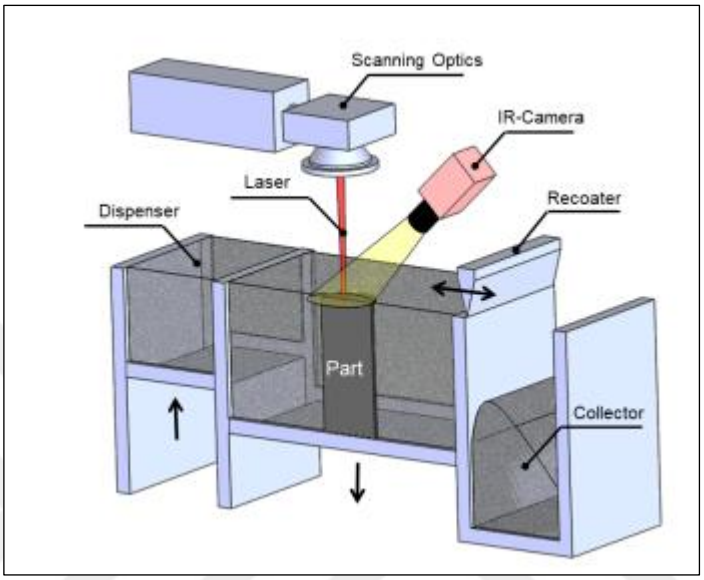

Figure 2.1. Selective laser melting technology schematic illustration **[2].**

Reduced lead times, greater material consumption efficiency, and lower tooling or mold investment costs are just a few benefits of the SLM process. Additionally, by significantly reducing the number of manufacturing processes, this method can improve the service life of the materials produced by doing away with joining operations brazing or welding and their damaging effects on the microstructure **[1]**.
However, the strong temperature gradient and quick solidification rate brought about by the SLM technique may cause several undesirable traits to show up in the microstructure of the manufactured parts. High residual stresses, the development of non-equilibrium phases, directed grain growth, the segregation of refractory materials, or the generation of defects like cracks and pores are some of the issues that might arise during the SLM processing. The mechanical characteristics and correctness of the components' dimensions and geometry can be greatly impacted by residual stress. To improve the qualities of materials and satisfy the demands of harsh working circumstances, post processing heat treatments are essential for getting rid of defects in manufactured parts. Furthermore, the unfavorable conditions during the SLM

process can be effectively reduced by preheating the powder bed or optimizing a process parameter [1].

2.2. Superalloys

High mechanical and corrosion resistance qualities are demonstrated by superalloys rich in VIII B group elements that were designed for high temperature applications. Such as industrial gas turbines, land vehicles, energy-producing facilities, the petrochemical industry, rocket engines, spacecraft, and heat exchangers all require superalloys that can operate under extremely high stresses and temperatures. Because superalloys maintain their strength even when exposed to elevated temperatures above 650°C for a long time **[3].**

Superalloy development from the 1940s to the present has focused on optimizing microstructures and refining manufacturing processes. Vacuum induction melting (VIM), developed in the 1950 years, increased the alloy's performance by regulating the chemical composition **[4].** During the 1960s, further progress came with directional solidification and single-crystal alloy manufacturing. These methods were specifically employed to produce engine components that minimized or eliminated grain boundaries oriented to the load direction. Currently, single crystal superalloys are progressively employed in gas turbine engine components, especially in applications requiring exceptional fatigue and creep resistance **[5].**

2.2.1. Classification of Superalloys

The most important factor in the structure-property connection of superalloys is their chemical composition. Superalloys are created by alloying iron, nickel, cobalt, and chromium in different proportions, resulting in distinct structures and characteristics that classify them into iron-nickel-based, cobalt-based, and nickel-based groups **[6].**

Figure 2. shows the stress stress rupture strength for the 3 types of superalloys.

a. Iron Based Superalloys

These alloys contain iron as the main element. In addition, they contain significant amounts of chromium, nickel and very small amounts of molybdenum or tungsten.

Iron-based superalloys are strengthened by carbides, intermetallic precipitates and/or solid-melts. The intermetallic precipitate is usually γ' (Ni3AlTi) phase. Phases precipitated due to alloying elements in the matrix with cubic face-centered lattice structure play an active role in determining the mechanical properties of the material. Iron-based superalloys are used up to temperatures of about 650ºC. The strength of these alloys is lower than nickel-based alloys. For this reason, nickel or cobalt based alloys are preferred when longer life and high mechanical and thermal strength are required at the same time. It is used in gas turbine engine blades, discs and shafts because it is cheaper than other superalloys **[7,8]**.

b. Cobalt Based Superalloys

Cobalt based superalloys containing cobalt as the main element are obtained by alloying with chromium, nickel, tungsten, carbon and other alloying elements. Cobalt based superalloys are strengthened by solid melt and carbide phases. None of the cobalt-based superalloys are complete solid-melt alloys because they contain secondary carbide phases or intermetallic compounds. This leads to ageing and loss of ductility at room temperature. These alloys have found use in parts that require long life at relatively low stresses and high temperatures **[6, 7]**.

c. Nickel Based Superalloys

For many high temperature applications, nickel based superalloys are outstanding materials because they have the best high-temperature strength of any superalloy category. At ambient temperature, these alloys have a stable austenitic FCC crystal structure; at increased temperatures exceeding 70% of their melting temperature, they have exceptionally high creep values. Either solid solution strengthening or precipitation hardening can be used to strengthen these alloys **[9,10,11]**.

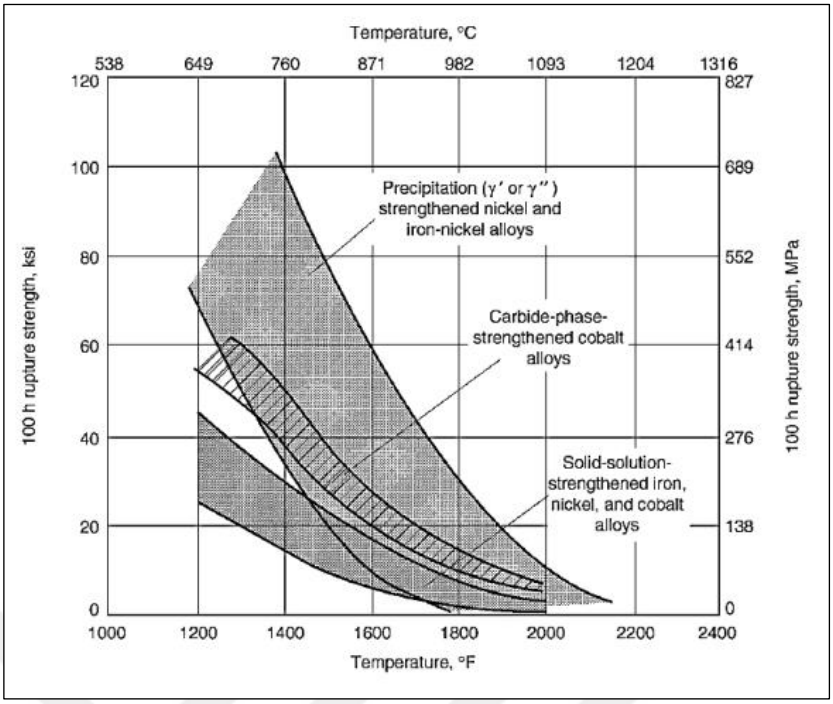

Figure 2.2. Comparison of stress-rupture tests of superalloys depending on their strengthening mechanisms **[1]**

2.3. Nickel Based Superalloys

The predominant constituent in such superalloys is nickel (30-70%), with a large quantity of Cr. Additionally contain less amount of aluminum, titanium, niobium, molybdenum, and tungsten to improve strength and corrosion resistance. Solid-solution and secondary-phase intermetallic precipitate phases strengthen nickel-based superalloys. Nickel, with its surface-centered cubic (FCC) crystal structure, exhibits tough and ductile properties due to its stability from 25°C to high temperature and absence of phase transformations. This stability prevents expansion and contraction conditions, ensuring microstructural stability at high temperatures.

2.3.1. Strengthening Mechanisms of Nickel-Based Superalloys

Superalloys have to be capable of sustaining at the high stress and temperatures without plastic deformation. Mostly, the increase in strength in metals is achieved by preventing dislocation movement. There are many ways to strengthen metals so that they have the desired mechanical properties. Among them, there are two most common mechanisms **[1]**:

a. Solid-Solution Strengthening

It is a nickel-based superalloy group designed to contain either none or small amounts of elements that will not form a secondary phase in its structure. Dislocation motion is prevented due to the mismatch of atomic radii and distortion of the crystal structure, leading to strengthening of the alloys **[1,12,13]**.

b. Precipitation Hardening

It is obtained by precipitating a second phase into the main matrix. The heat-treated alloys are strengthened by these precipitates, which interact with dislocations within the matrix. The mechanisms behind precipitation hardening primarily depend on two scenarios related to the critical size of the particles. When precipitates are smaller than the critical size, dislocations can cross the obstacles. Conversely, if precipitates exceed the critical size, dislocations can propagate around the particles, leaving dislocation loops. In both scenarios, the mechanical strength of the superalloy are negatively impacted, resulting in a decrease in yield strength. So, the precipitates size should be sized appropriately to prevent dislocations from passing through them, whether by cutting through or bowing around the obstacles **[1,12,13]**.

In general Nickel superalloys; By adding Al, Ti and Nb elements, γ' (Ni_3 (Al, Ti)) and γ" (Ni_3Nb) phases are precipitated in the structure, resulting in increased strength. The strengthening behavior of heat-treated alloys is largely determined by the specific attributes of the precipitates, including their shape, distribution, and volume fraction, along with the level of coherence between the precipitates and the surrounding matrix. **[1,12,13]**.

2.3.2. Phases of Nickel-Based Superalloys

The microstructure of superalloys generally features a gamma (γ) matrix phase with gamma prime (γ'), gamma double prime (γ") and intermetallic compounds, as well as metal carbides or borides [10].

Phases formed in nickel based superalloys and the properties of these phases;

a. Gama (γ) Phase:

The predominant element in the FCC γ-matrix phase is nickel, with significant concentrations of solid solution elements such as cobalt, chromium, molybdenum, and iron. The matrix phase is well-suited for high temperature alloys because of its high modulus and numerous slip systems, which contribute to superior tensile strength, fatigue resistance, and creep performance **[11]**.

b. Gama Prime (γ'):

Result of the addition of Aluminum and Titanium elements for high temperature strength and creep deformation, a γ' (Ni_3 (Al, Ti)) intermetallic phase compatible with the γ matrix in the austenitic structure is obtained. While this intermetallic phase has a spherical structure at low Al and Ti amounts, it has a cubic structure at high additions. This change is attributed to the γ/γ' lattice mismatch **[14,15]**.

c. Gama Double Prime (γ"):

As a result of the addition of the Nb element, which is seen in Iron and Nickel-based superalloys, a γ" (Ni_3Nb) precipitate phase with a body centered tetragonal (HMT) structure is formed. It is a precipitate phase that is semi-compatible with the matrix. Generally, in superalloys such as Inconel 718, γ' and γ" phases precipitate together into the γ matrix **[14]**.

d. Delta (δ) Phase

It is a phase with an orthorhombic structure and the composition of Ni3 (Nb). It precipitates at grain boundaries, increasing grain boundary strength and fatigue life. Excessive amounts negatively affect the material by causing brittleness in the structure **[16]**.

e. Topologically Close-Packed Phases

Formed in certain compositions and under certain conditions; They are phases with plate-like or needle like morphology such as σ, μ and Laves. They generally nucleate at grain boundaries, causing a decrease in tensile strength and ductility. These phases; By binding the precipitated phases to themselves, they cause a decrease in creep strength and a decrease in rupture strength due to their brittle structure **[14]**.

f. Carbides

Carbon is added in the amount of 0.2-0.02% to combine with reactive metals such as Titanium, Tantalum, Hafnium and Niobium in the structure to form MC type metal carbide. These MC type carbides tend to form carbides such as $M_{23}C_6$ and/or M_6C at grain boundaries during the heat treatment process. Carbide precipitates form discontinuously and irregularly along grain boundaries. These structures provide properties that increase the tensile strength under high temperature service conditions **[14,15]**.

2.3.3. Inconel 718 Superalloys

Inconel 718 superalloy; It is one of the nickel-based superalloys developed by the International Nickel Corporation in the 1950s and continues to be used in many areas, especially gas turbine engines in aviation **[17]**.

Inconel 718 on γ matrix; There are γ' (Ni_3 (Al, Ti)), γ" (Ni_3 Nb) and δ precipitate phases. Among these phases, it is the Niobium-rich metastable γ" precipitate phase with the HMT (body-centered tetragonal) structure that provides the main strength. This instability arises from matrix/precipitate lattice incompatibility. Generally the application temperature is 650 °C. After this temperature, the strength generally decreases by turning into the γ"→δ phase **[17]**.

Figure 2 presents microstructural images illustrating the phases of Inconel 718. The delta phase appears as a brittle, needle-like structure. γ' and γ" phases are dispersed throughout the matrix, with an approximate size of 50 microns. γ" has a more elongated and thin form, gamma prime tends to be more rounded. The Laves phase is observed both within the matrix and along the grain boundaries **[22]**.

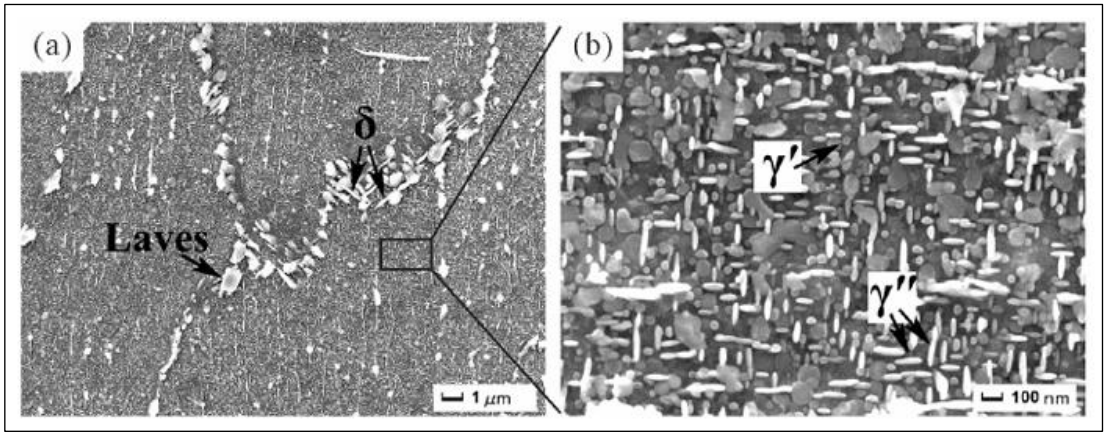

Figure 2.3. Phases of IN 718

In the following paragraphs, the studies of IN718 superalloy produced by additive manufacturing in the literature are described.

Xu et al. in their study, investigated the effects of various post-processing techniques, such as hot isostatic pressing (HIP), heat treatment (HT), and their combination (HIP+HT), on the microstructural and mechanic properties of IN718 superalloy produced via laser powder bed fusion (LPBF). The microstructural evolution was thoroughly analyzed using techniques like SEM, TEM, STEM, and XRD. The findings revealed that HIP effectively dissolve the Laves phase and assisted the formation of fine γ″ precipitates, while HT led to the development of larger γ″ precipitates. The HIP+HT process resulted in the highest yield strength, but a significant reduction in ductility was observed after both HT and HIP+HT treatments. This reduction in ductility was attributed to the increased size of γ″ precipitates, which restricted dislocation movement, and the precipitation of δ phase at grain boundaries, which created stress concentration sites prone to crack initiation. Although the finer and more uniform distribution of γ″ precipitates in HIP+HT condition slightly improved ductility, the overall increase in material hardness contributed to the observed loss in ductility **[23]**.

Zhang et al. in their study, investigated the effects of standard heat treatments on the microstructural and mechanic properties of IN718 superalloy manufactured through SLM. The researchers applied two standard heat treatments: solution and aging (SA); homogenization, solution, and aging (HSA). The results revealed fine dendritic structures, Laves phases and carbide particles in the as built samples, while the heat

treatments resulted in the substitution of these structures with recrystallized grains. It was found that strength and hardness values of the heat treated samples increased significantly, although there was a considerable reduction in ductility. This decrease in ductility was attributed to the precipitation of γ′ and γ″ phases in the matrix, which restricted dislocation movement, as well as the formation of needle-like δ phases at grain boundaries that acted as crack initiation sites **[24]**.

Diepold et al. in their study, investigated the optimization of heat treatment for additively manufactured Ni-base superalloy IN718. The goal was to enhance the microstructure and mechanical properties of the alloy. They used SLM to produce samples and conducted various heat treatments including solution heat treatments (SHT) at different temperatures (930°C, 954°C, and 1000°C) followed by aging. Compression tests applied. The results showed that higher SHT temperatures lead to the dissolution of the Nb-rich Laves phase and reduced dislocation density, improving the alloy's strength. The study concluded that SHT at 1000°C, which avoids δ-phase precipitation, resulted in the optimum strength due to higher γ′ and γ″ volume fractions **[25]**.

The aim of the study conducted by Zhang et al. is to investigate effect of microstructure on the high-temperature stress rupture properties of IN718 alloy fabricated via SLM. In the study, SLM built specimens underwent hot isostatic press, solution treatment, and aging processes, and their microstructure and stress rupture were analyzed. The results indicate that as the size of γ″ precipitates increases, the rupture life extends, while regions with fine grains exhibit a higher density of geometrically necessary dislocations. This implies that fine grains undergo more intense plastic deformation in order to accommodate the uneven strain imposed by the neighboring coarse grains. The stress concentration is greater in fine-grain regions, making these areas more prone to initiation and propagation of micro cracks. Furthermore, the increase in γ″ precipitate size with aging time leads to a shift in deformation mechanisms: specimens with smaller γ″ precipitates exhibit dislocation slipping and micro-twinning modes, while those with larger γ″ precipitates predominantly show dislocation slipping and isolated faulting modes **[26]**.

In their study Kuo et al. aimed to investigate the effect of post-processes on the microstructure and creep properties of IN718 fabricated by SLM. The experimental method involved fabricating IN718 specimens using SLM, followed by various post-

processing techniques, including heat treatments and HIP. The results showed that recommended HT (STA-980°C) was ineffective for SLM-processed specimens, leading to uneven grain sizes and high dislocation densities. However, the HIP + direct aging process significantly improved the creep behavior at 650 °C, extending the creep rupture life to approximately 800 hours by eliminating pores and preventing microcrack nucleation. The study concluded that suitable post-processing is crucial for enhancing the mechanic properties of SLM-fabricated IN718 **[27]**.

Gao et al. in their study investigated the high temperature mechanical strength of SLM-fabricated IN718 alloy under various heat treatments. The researchers used SLM to fabricate specimens and applied different heat treatment schemes (SHT 980, SHT 1080, and SHT 980 + 1080). They conducted tensile and stress rupture tests at 650°C to evaluate the mechanical performance. The results showed that the SHT 980 + 1080 condition offered optimal high temperature mechanical properties, with the morphology and distribution of the δ phase in the γ matrix being crucial. The study concluded that a moderate presence of δ phase along grain boundaries enhances high-temperature mechanical strength by balancing dislocation motion and stress concentration **[28]**.

Shi et al. in their study was investigated the microstructural and creep anisotropy of IN718 alloy processed by SLM. Cylindrical rods were fabricated with their axes either normal or parallel to the building directions, then homogenized and double aged. Creep tests were conducted under a constant stress of 650 MPa at 650 °C. The results showed that both equiaxed grains and columnar dendrites existed in the samples before and after creep, with grain sizes remaining nearly unchanged. The vertical specimen demonstrated an extended creep rupture life (approximately 120 hours), attributed to its larger grain size, fewer transverse grain boundaries, and a higher volume fraction of γ″ phases. Stress concentration at transverse grain boundaries led to intergranular fracture in both orientations. The study concluded that the anisotropy of creep behavior could not be eliminated by the current heat treatment process [29].

The difference of our study from the literature is that the temperature (650°) & load (689MPa) at which the mechanical properties are examined is high and this temperature & load is not studied in the literature. In addition, the effect of the laves phase is investigated in detail.

3. EXPERIMENTAL PROCEDURE

3.1. Casting, Powder Atomization and SLM Manufacturing of Inconel 718

In718 superalloy ingots were cast at Tubitak MAM Metallic Materials Technology Research Center for the gas atomisation process. The ingots were pulverised using the gas atomisation method by Sentes1 company. This domestically produced IN718 powder used for the starting materials of SLM process.

The manufacturing of the In718 superalloy samples carried out under argon atmosphere that preventing to oxidation and EOS M290 was used to manufacturing samples. Furthermore, the platform was heated to 80 ºC to minimize the temperature difference between the platform and the produced components (**Table 3.1**). Cylindrical bars were produced with the axis of the cylinder perpendicular to the building direction. Figure 3.1 shows the building direction of the cylindrical bars.

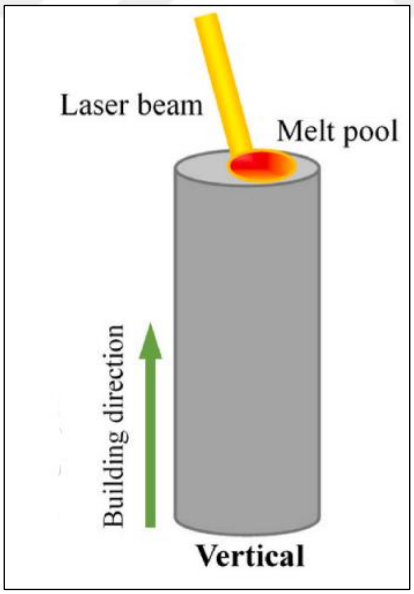

Figure 3.1 . The building direction of the cylindrical bars **[19]**

Table 3.1. SLM Manufacture Parameters

SLM Manufacture Parameters	Value
Layer Thickness	0.04mm
Volumetric Energy Density	67.47 J/mm3
Substrate Temperature	80°C
Inert Gas	Argon

3.2. Heat Treatment

Different heat treatments were applied to observe their effects on the microstructure and mechanical properties. The design of the two different heat treatments was conducted using the ThermoCalc software and DSC analysis. The primary goal of these heat treatments is to dissolve the brittle Laves phase within the matrix, disrupt the melt pool structure, and form strength-enhancing phases during aging. Additionally, for comparison, the standard heat treatment (SHT) specified by EOS for IN718 superalloy produced by additive manufacturing was applied. In this study, while optimizing the heat treatment, solution annealing temperatures were varied, keeping the aging time and temperatures constant. Solution annealing treatments were performed in a Protherm box furnace, and aging treatments were carried out in a Nabertherm box furnace under an argon atmosphere. The heat treatments applied to IN718 are detailed in **Table 3.2.**

Table 3.2. Heat treatments applied to IN718

Heat Treatment	Homogenisation	Solutionizing	Aging
As Built	-	-	-
Standard Heat Treatment (SHT)	-	954°C/1h	720 °C/8 h FC - 620 °C/8 h AC
HT1045	1045°C/1h	954°C/1h	720 °C/8 h FC - 620 °C/8 h AC
HT1090	1090°C/1h	954°C/1h	720 °C/8 h FC - 620 °C/8 h AC

3.3. Simulation Studies

Thermo-Calc Software and databases enable thermodynamic calculations, providing a deeper understanding of material properties. Thermo-Calc TCNI11 was used to

calculate the solidification diagrams and binary phase diagrams of In718 via using the Nickel based superalloys TCNI11 database.

3.4. Characterization Studies

3.4.1. Metallographic Sample Preparation

The samples were cutted by abbrasive cutter and mounted by hot mounting machine. The samples were grinded using 240, 320, 600, 800, 1200, 2500 SiC grinding papers, respectively. And polished with diamond suspension 6 μm and 1 μm. Then the samples were electrically etched with Kalling's reagent for 5-10s under 3A using Struers Lectropol-5. Optical micrographs were taken with an Olympus Preciv microscope after etching.

3.4.2. Scanning Electron Microscope (SEM)

A Scanning Electron Microscope (HITACHI SU7000) was used to observe the changes in the microstructure of the heat treated samples compared to as built. And also, The samples' chemical composition was identified and observed changes of the phases through the Energy Dispersive spectroscopy (EDS) detector attached to the SEM.

3.4.3. XRD

Phases of the microstructure of the as-built condition and after various heat treatment processes were analyzed using XRD. Rigaku X-Ray Diffractometer was used Cu-Kα radiation with 30 mA and 40 kV and 2θ between 20°- 120° with scan speed of 1°/min.

3.4.4. DSC

Differential scanning calorimetry (DSC) was utilized to detect the key temperature ranges at which secondary phases either dissolve or form precipitates. In a Setaram DSC/TGA, cylindrical samples measuring 3 mm in diameter and 10 mm in height were placed into alumina crucibles and heated to a maximum temperature of 1400 ◦C. The heating rates for this process was 10 ◦C/min and 20 ◦C/min.

3.5. Mechanical Test

3.5.1. Creep Test

Creep test was performed according to the ASTM E139 standard and tests were performed at 650°C under 689MPa load. The load value, which has not received much attention in the literature, and the working conditions of the IN718 superalloy were taken into consideration while choosing the test parameters. For every test condition, two creep rupture test applied to guarantee the correctness of the findings.

3.5.2. High Temperature Tensile Test

A high-temperature tensile test, following ASTM E21 guidelines, was conducted to examine material properties such as tensile strength, yield point, strain at break and reduction of area under high-temperature conditions. The technical drawing of the tensile test samples.

High temperature tensile test were applied at 650°C and for every test condition, two tensile testing applied to guarantee the correctness of the findings.

Thermocouples were fixed to the top, bottom, and center of the gage length of the samples, and they were used to measure the temperature of the heating process which took place in a furnace. Extensometers that were directly linked to the samples were also used to measure strain.

4. RESULTS & DICUSSION

4.1. Microstructural Characterization

4.1.1. As-Built

The samples that were classified as vertically constructed (VB) samples had longitudinal axes that were perpendicular to the construction platform. **Figure 4.1** shows clear view of the melt pool morphology in the lateral direction that shows arc-shaped characteristics. Melt pool microstructure is common microstructure of additively produced part with selective laser melting (SLM) process. And also the laser scanning paths can be shown on the axial observation direction **Figure 4.2.**

Figure 4.1. Microstructure of the melt pool morphology

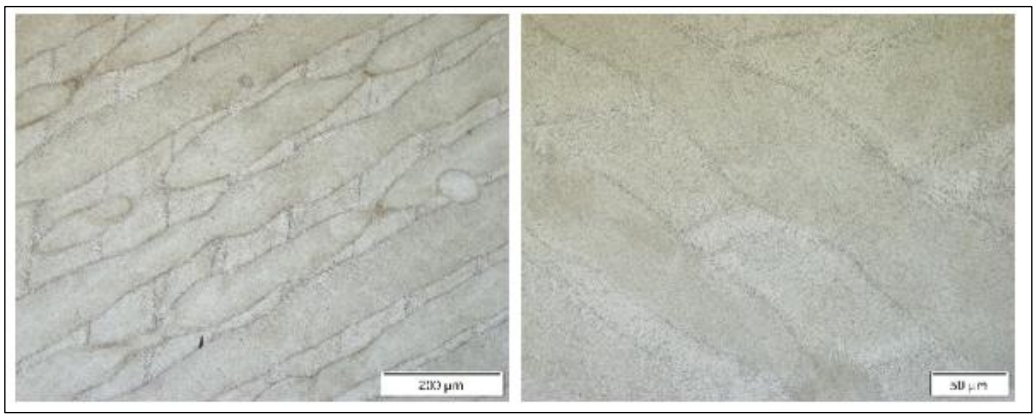

Figure 4.2. Microstructure of the melt path morphology

Figure 4.3 shows SEM images of as built microstructure of SLM. The operating mechanism of the slm process is rapid heating and rapid cooling. During this rapid solidification, heavy elements such as Nb and Mo do not have time to diffuse and segregate and formed Nb-rich laves phase. Laves phase is a brittle phase and causes deterioration of mechanical properties such as fatigue and creep. The gamma double prime phase, which provides strength in In718, also contains a high proportion of Nb. The presence of the laves phase reduces the Nb in the matrix and therefore restricts the formation of gamma double prime. For this reason, laves phases are dissolved by heat treatment and gamma double prime is formed. In the white areas seen in Figure 4.3 is Nb-rich laves phases according to the EDS analysis given in **Table 4.1**.

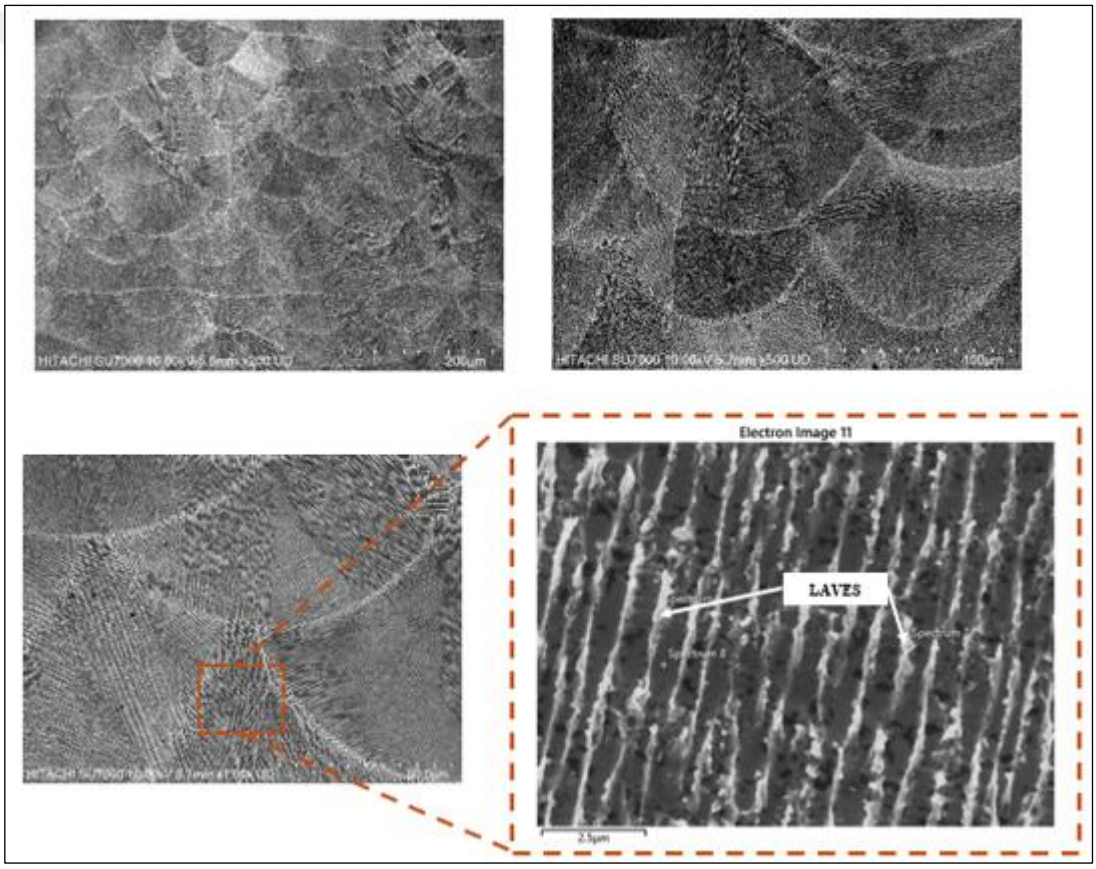

Figure 4.3. SEM images of As Built Microstructure In718

Table 4.1. EDS analysis of as built SLM IN718

Spektrum	Ni	Cr	Fe	Nb	Mo	Ti	Al	Phase
6	50.4	20.1	16.7	8.9	2.7	0.9	0.3	**Laves**
7	51.2	15.3	14.1	14.5	3.8	0.8	0.3	**Laves**
8	53.7	17.5	19.8	3.9	4.0	0.8	0.3	**Matrix**
9	50.4	22.0	18.9	5.4	2.1	0.8	0.4	**Matrix**
10	48.6	21.3	20.7	5.6	2.4	1.0	0.5	**Matrix**
11	53.7	19.6	17.8	5.2	2.8	0.5	0.4	**Matrix**
12	50.1	20.9	20.8	4.4	2.5	0.8	0.5	**Matrix**

4.1.2. Heat Treated

Heat treatments primarily aim to dissolve the brittle Laves phase in the matrix, disrupt the melt pool structure, and develop strength-enhancing phases during the aging process. So determine the critical temperature like precipitation and dissolution DSC analyses and ThermoCalc Studies carried out.

DSC (Differential Scanning Calorimetry) analysis is an essential technique used to investigate the thermal properties and phase transitions of materials. The main reasons for conducting DSC analysis include:

1. **Phase Transitions**: To determine phase changes such as melting, crystallization, and sublimation in the material.
2. **Thermodynamic Properties**: To measure thermodynamic characteristics such as enthalpy and heat capacity.
3. **Stability Assessment**: To evaluate the stability of materials against temperature variations and identify degradation temperatures.
4. **Alloy Characterization**: To examine properties such as aging processes and precipitation behavior in metal alloys.

For these reasons, DSC analysis is widely utilized. Figure 4.4. illustrates the signals obtained from heating rates conducted on the as built samples at various heating rates It is noteworthy that as the heating rates increase, the peaks exhibit a slight shift towards higher temperatures and become more distinct. The most prominent peaks were utilized to determine the thermodynamic transformations occurring in the material.

As observed, the heating ramp reveals three exothermic peaks and one endothermic peak, which are marked with arrows. These peaks correspond to the precipitation of γ' at 520 °C, γ″ at 702 °C, and δ at 940 °C. Conversely, the endothermic peak occurring around 1050 °C signifies the dissolution of pre-existing metastable Laves phases.

It is also observed in the literature that the formation temperatures of the phases are approximately at these temperatures **[20,21]**. Table 4.2 shows important critical temperatures.

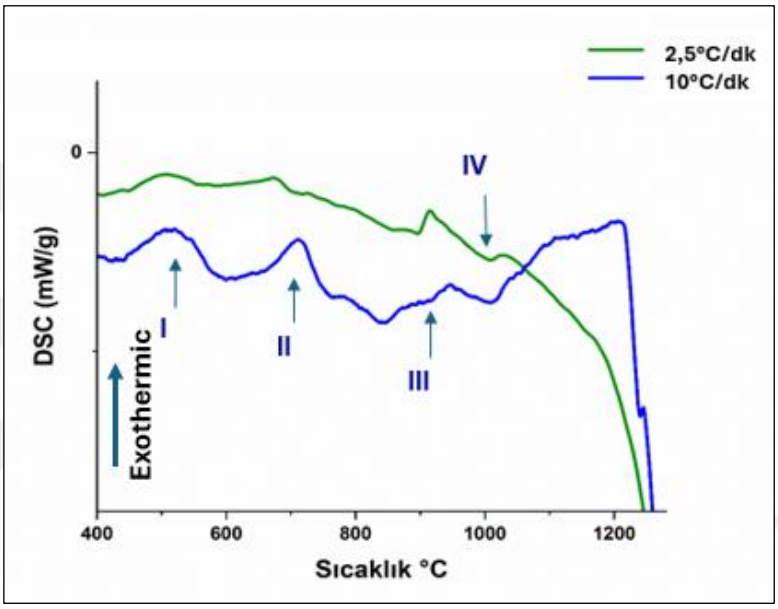

Figure 4.4. DSC analysis of IN718

Table 4.2. DSC analysis results of IN718

Temperatures		
I	520,93°C	γ´ precipitation
II	702,50°C	γ'' precipitation
III	940,60°C	δ precipitation
IV	1050°C	Laves dissolution

The chemical composition of In718 was input the Thermocalc software, and a phase diagram was generated. The Ni-based thermodynamic database TCNI11 is utilized for calculating Scheil's plot and the fraction of phases against temperature plot. Figure 4.5 shows the phase diagram generated by ThermoCalc analyses and Table 4.3 shows important critical temperature.

The software's Scheil module estimates the phase transformations during solidification and calculates the redistribution of solutes between the solid phase and the solidifying liquid. Figure 4.5.(c) illustrates the expected phases and their corresponding formation temperatures during solidification. The temperature at which solidification occurs is estimated to be 1340°C, with the gamma matrix forming within the dendrite core. As solidification progresses, NbC, laves, delta, gamma prime phases are predicted to form in the gamma matrix, respectively. As solidification continues, it leads to the formation of delta phase in the interdendritic regions.

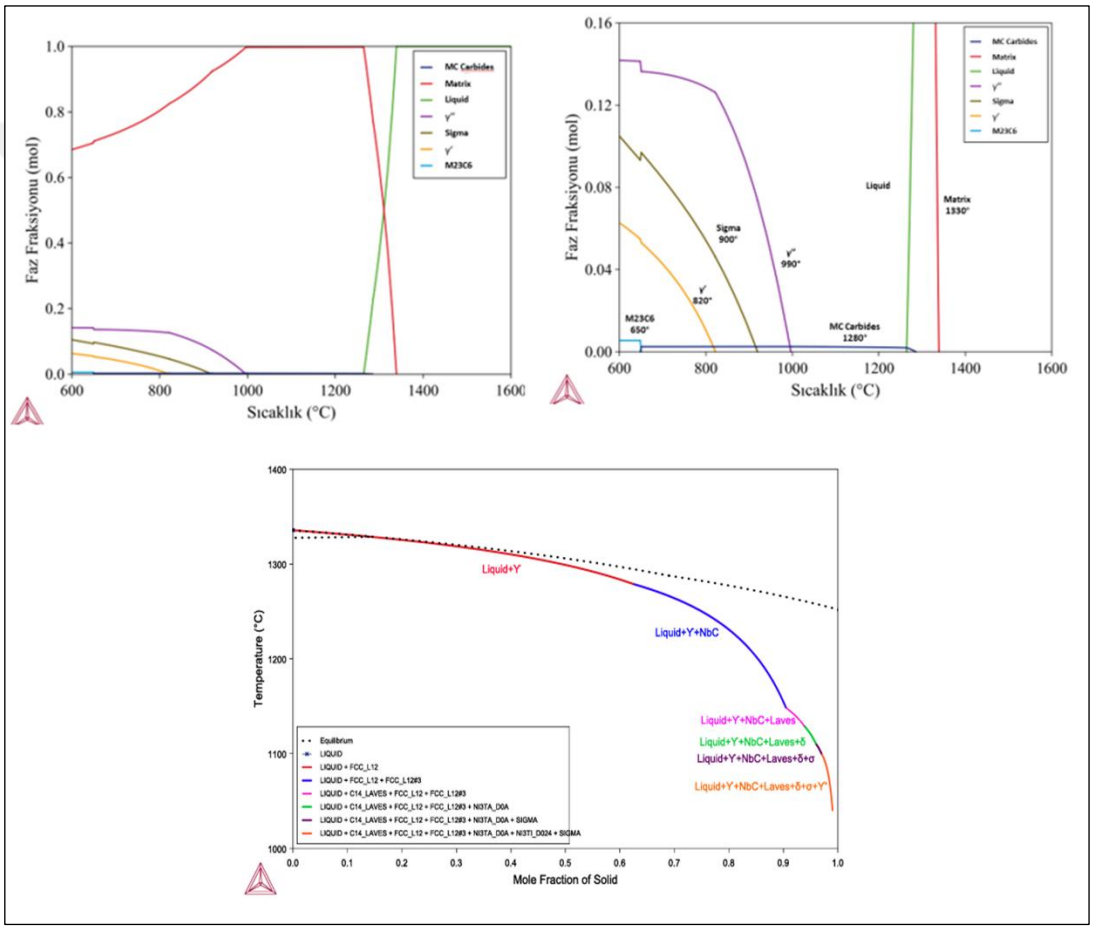

Figure 4.5. ThermoCalc analysis of IN718

Table 4.3. Important critical temperature of Inconel 718.

Phases	Temperature
Matrix	1330°C
MC Carbides	1280°
Delta	990°
Sigma	900°
Gamma Prime (γ')	820°
M23C6	650°

Heat treatment design was carried out to see the effect of the formation of strength enhancing phases formed during aging in terms of microstructural and mechanical properties by applied solution heat treatment below and above the dissolution temperature of Laves phase. Microstructures of heat treated samples schedule shown Figure 4.6, Figure 9, Figure 11.

Figure 4.6 show SHT optical microscope images and Figure 4.7 SEM analyses. After heat treatment laves and delta phases seen in EDS analyses in Table 4.4. The dispersion of laves phase after the solution heat treatment and the formation of γ' and γ'' during ageing is expected. However SHT heat treatment was not sufficient for the eliminate of the laves phase. And also seen in the SEM images delta phases that brittle phases also. Laves and delta phases formed at the grain boundary.

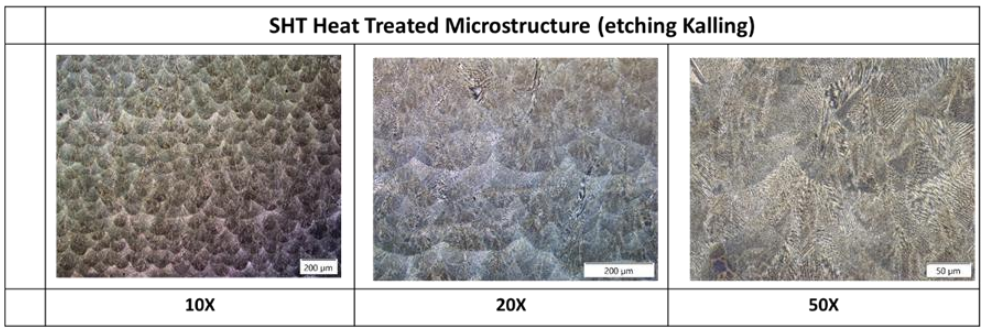

Figure 4.6. Microstructure of Standard Heat Treatment (SHT)

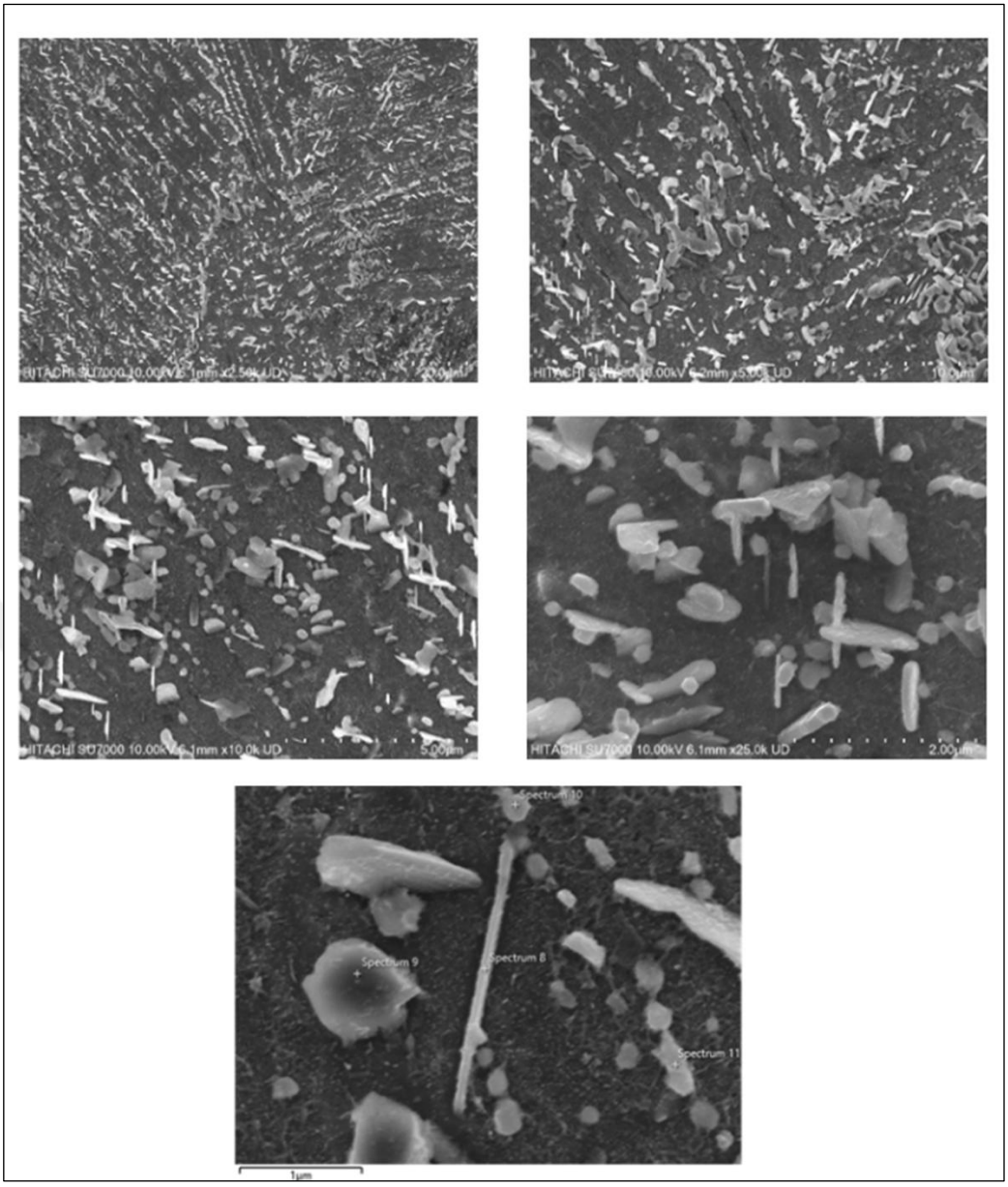

Figure 4.7. SEM images of SHT of IN718

Table 4.4. EDS analysis of SHT of SLM IN718

Spektrum	Ni	Cr	Fe	Nb	Mo	Phase
8	62	14	10	15	1	**Delta**
9	39	16	15	19	10	**Laves**
10	53	23	19	10	6	**Laves**
11	53	23	18	10	5	**Laves**

Figure 4. shows laves and delta phases formed at the grain boundary. High magnification of the SEM images seen γ′ and γ′′ on the literature. In the Figure 4.8 a) thesis SEM images b) literature SEM images **[17]**.

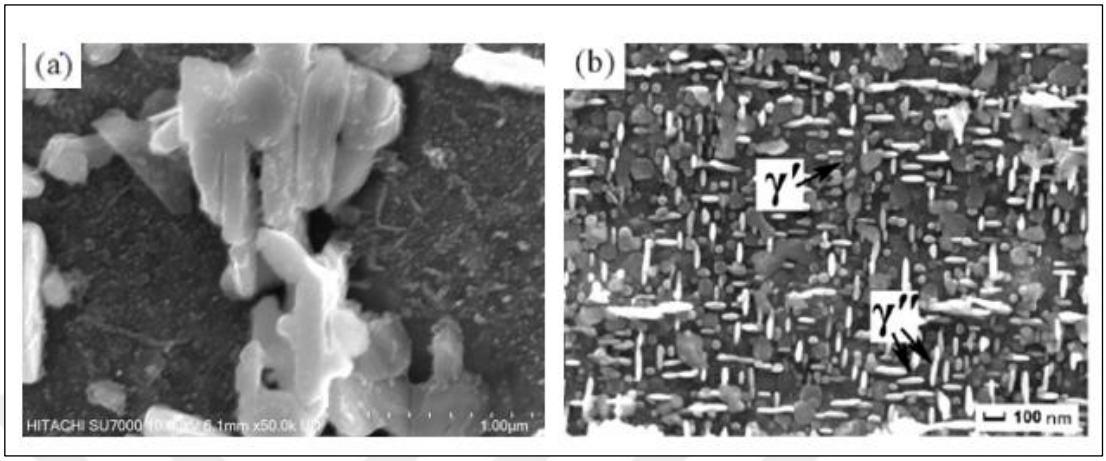

Figure 4.8. a) Thesis SEM image **b)** literature SEM image of SLM In718 **[17]**

Figure 4.9 shows microstructure of HT1045 optical microscope images. The melt pool structure is completely dispersed and there are no traces of additive manufacturing. Homogenous and equaxed grains are obtained. Annealing twins and recrystallised grains were observed.

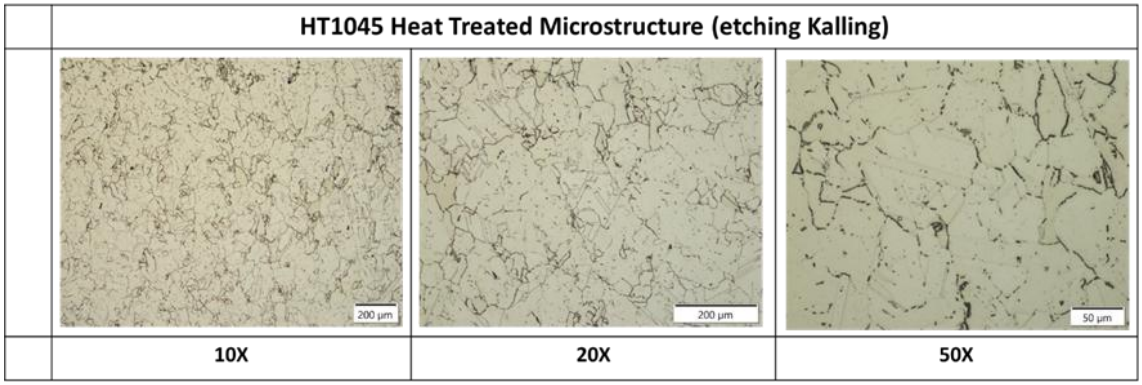

Figure 4.9. Microstructure of HT1045

Figure 4.10 shows SEM images and EDS analyses of HT1045 (Table 4.). At high magnification of the SEM images seen gamma prime and gamma double prime. Laves phase exist at the grain boundary, they are not dissolve completely.

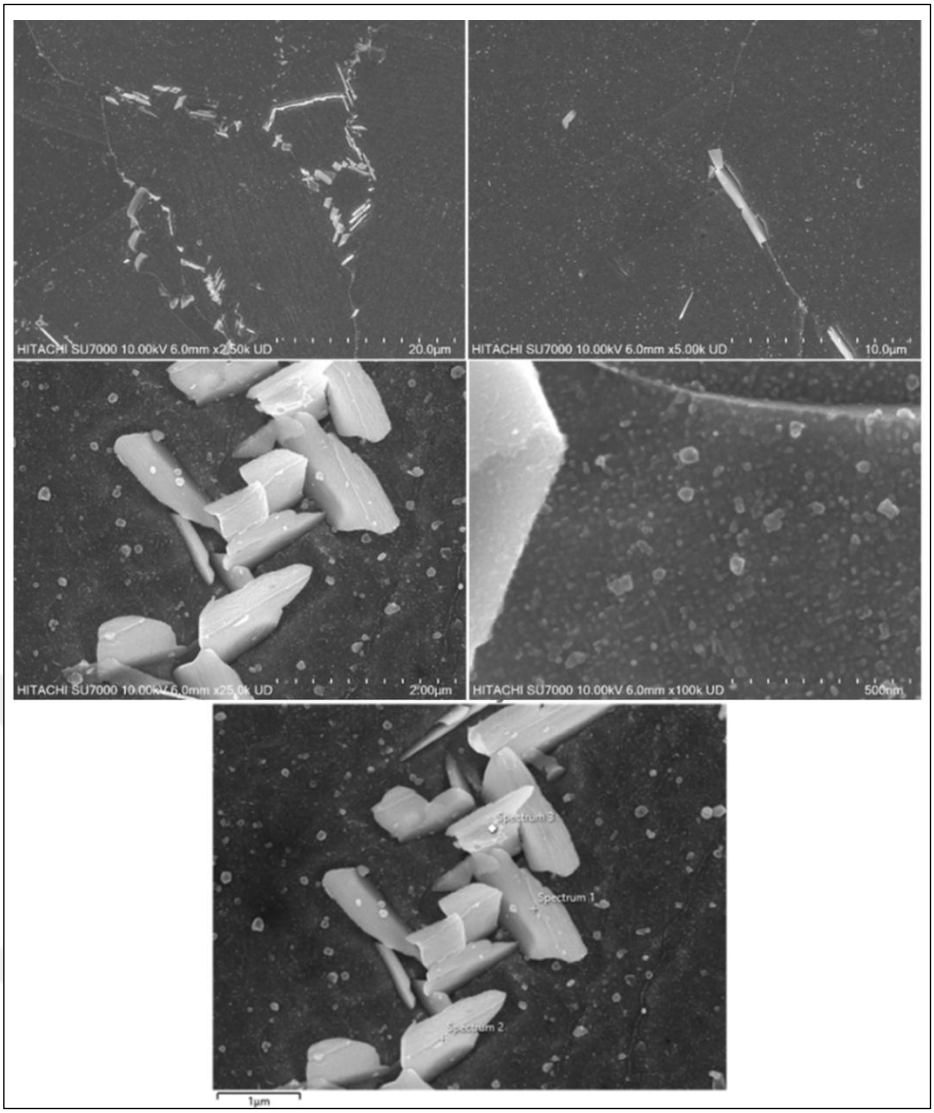

Figure 4.10. SEM images of HT1045 of IN718

Table 4.5. EDS analysis of HT1045 of SLM Inconel 718

Spektrum	Ni	Cr	Fe	Nb	Mo	Ti	Al	Phase
1	54.4	18.0	13.5	10.2	2.0	1.6	0.3	Laves
2	55.1	12.5	9.3	14.7	4.1	3.8	0.4	Laves
3	60.8	10.5	6.9	17.3	1.7	2.4	0.3	Laves

Figure 4.12 and **Figure 4.12** shows microstructure of HT1090 heat treatment's optical microscope and SEM images . The melt pool structure is completely dispersed and there are no traces of additive manufacturing like heat treatment HT1045. Homogenous and equaxed grains are obtained. Annealing twins and recrystallised grains were observed.

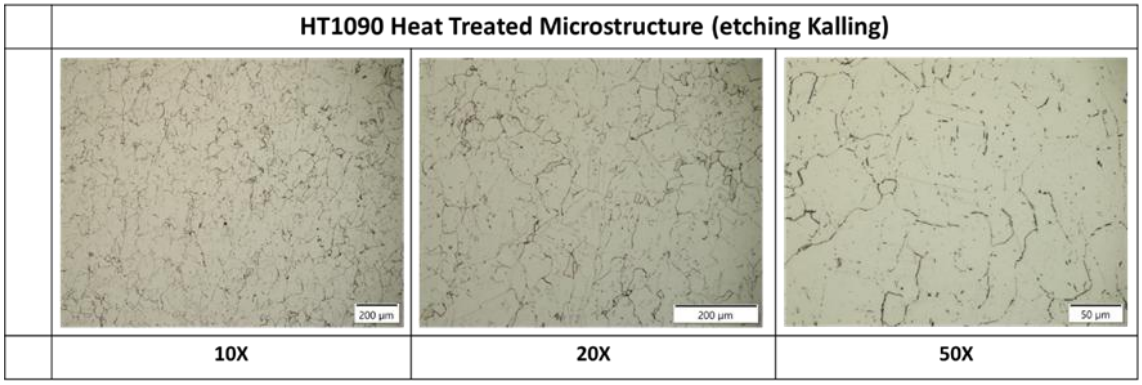

Figure 4.11. Microstructure of HT1090

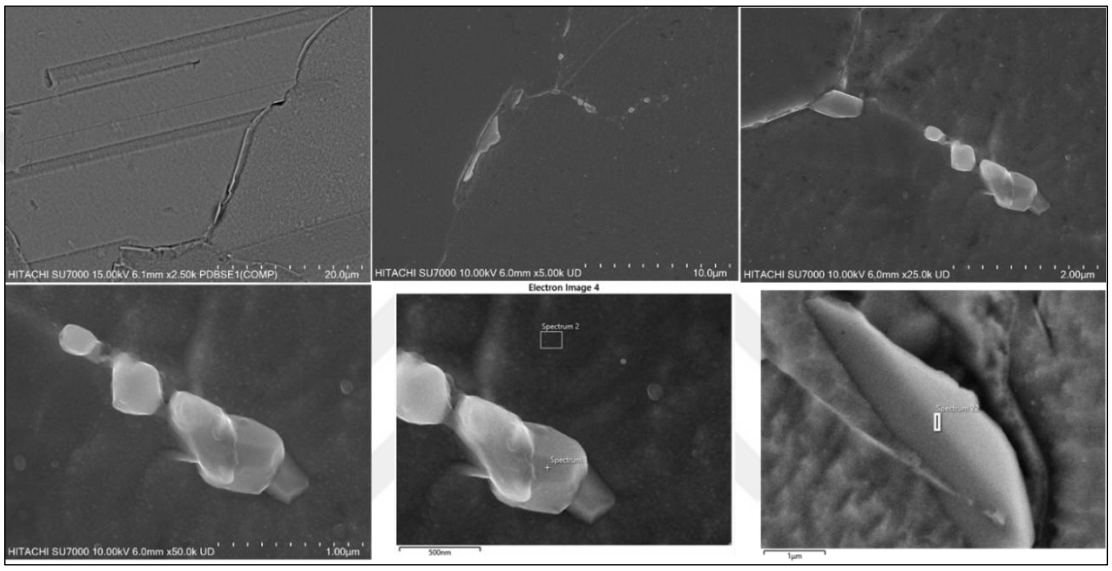

Figure 4.12. SEM images of HT1090 of IN718

Table 4.6. EDS analysis of HT1090 of SLM IN718

Spektrum	Ni	Cr	Fe	Nb	Mo	Ti	C	Phase
1	36.1	13.2	12.4	14.1	1.8	1.7	19.8	NbC
2	52.5	20.6	20.2	3.7	2.4			Matrix
3	59.0	13.1	12.8	10.2	2.9	1.5		Laves

4.2. Mechanical Characterization

With the dissolution of the Laves phases, the matrix phase was enriched in niobium. γ′ and γ″ phases were formed in aging heat treatment. These phases prevented dislocation movements and increased the creep life. As Built state has orientated grains. The cracks formed in the creep test started at the boundaries of the orientated grains.

In SHT heat treatment, an inhomogeneous microstructure was observed in which the oriented grain structure and melt pool structure were not completely dispersed.

In addition more equiaxed, homogeneous grain structure was formed in HT1045 and 1090 and the melt pool morphology disappeared completely. It was also observed that annealing twinning occurred after heat treatment.

They are phases with plate-like or needle-like morphology such as σ, μ and Laves. They generally nucleate at grain boundaries, causing a decrease in tensile strength and ductility. These phases; By binding the precipitated phases to themselves, they cause a decrease in creep strength and a decrease in rupture strength due to their brittle structure.

4.2.1. High Temperature Tensile

A high-temperature tensile test was conducted to examine material properties such as tensile strength, yield point, strain at break and reduction of area under high-temperature conditions. Figure 4.10 and table 4.10 shows high temperature tests results. The tensile tests at high temperatures (650°C) revealed that as-built Inconel 718 has a lower yield strength but higher elongation compared to heat-treated samples. n the as-built condition, the rapid cooling rate of the SLM process leads to a fine dendritic microstructure and limited precipitation of strengthening phases like γ' and γ''. This fine structure allows for greater plastic deformation, making the material more ductile. However, without sufficient γ'' and δ phase precipitation, the yield strength remains low because there is less resistance to dislocation motion. Additionally, Laves phases that form in the as-built state do not contribute to strengthening and can even be detrimental to mechanical properties, further lowering the yield strength.

The heat-treated specimens, especially under the HT1090 + HT1045 condition, showed a significant improvement in tensile and yield strengths but a reduction in ductility. The reason for this is that the heat treatments promoted the formation of γ' and γ'' strengthening phases and controlled the distribution of the δ phase. These strengthening phases increase resistance to dislocation motion, thereby raising tensile strength but reducing elongation. Meanwhile, excessive δ phase formation, sufficient dissolution of laves phases as in the SHT condition, led to dislocation pile-ups and early failure due to microcracks. Although the yield strength increases relatively in the SHT heat treatment, ductility is quite low due to the brittle delta phase formed.

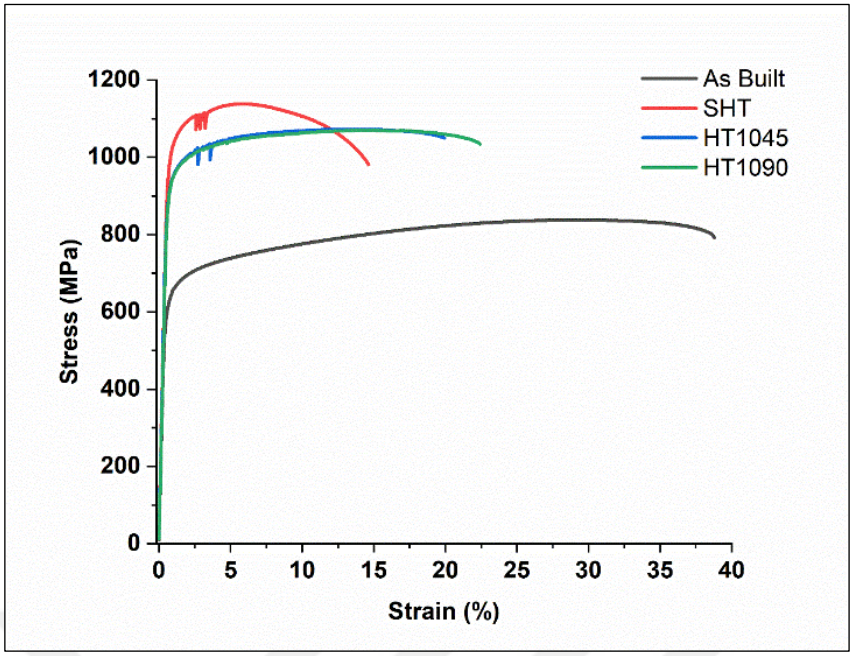

Figure 4.23. High Temperature Tensile Test Results

Table 4.7. High Temperature Tensile Test Results

Hot Temp. Tensile Test	m_E (GPa)	$R_{p0.2}$ (MPa)	R_m (MPa)	Elongation (%)
As Built	154,317	606,478	837,445	38,303
SHT	177	985	1138	14,1
HT1045	172	908	1072,428	19,75
HT1090	163	914	1070	21,97

4.2.2. Creep Test

The as built Inconel 718 alloy exhibited the shortest creep rupture life, 65 hours. This indicates the material's poor high-temperature strength in the as-built state, which is attributed to the insufficient γ' and γ'' phases, along with a fine-grained structure and the presence of Laves phases. These Laves phases, along with voids at the grain boundaries, likely contributed to crack initiation, leading to premature failure. In contrast, heat-treated samples showed significantly longer creep rupture lives. For example, the **SHT** condition resulted in a creep rupture life of approximately 95 hours, while the **HT1045** condition reached around 118 hours. The **HT1090** condition achieved the highest creep rupture life, at 137 hours. This notable improvement is due to the stabilization of the microstructure following heat treatment. In the as-built state, the fine-grained structure provides high strength at room temperature, but at elevated

temperatures, grain boundaries weaken, accelerating grain boundary sliding and failure. Heat treatment, particularly under **SHT** conditions, strengthens the grain boundaries through δ phase precipitation, which slows grain boundary sliding and enhances the high-temperature strength of the material. However, the excessive δ phase in the SHT condition, combined with the presence of brittle Laves phases, limits further improvement in creep rupture life. Figure 4.11 and table 4.11 shows creep tests results.

During heat treatment, harmful Laves phases in the as-built samples dissolve, releasing niobium (Nb), which becomes available for the precipitation of γ' and γ'' phases. These strengthening phases hinder dislocation movement, increasing the material's strength. In the **HT1045** condition, incomplete dissolution of the Laves phase limited the optimal precipitation of γ' and γ'' phases. Nonetheless, the controlled δ phase distribution along grain boundaries contributes to the improved creep rupture life.

In the **HT1090** treatment, most of the Laves phases dissolved, increasing the Nb content in the matrix, which in turn enhanced the volume fraction of γ' and γ'' phases. Additionally, δ phase precipitation was observed at grain boundaries in a controlled manner, providing a pinning effect that restricted grain boundary sliding and dislocation movement. This process delayed deformation at high temperatures, significantly extending the creep rupture life.

The more homogeneous and equiaxed grain structure formed in the **HT1045** and **HT1090** conditions further contributed to the superior creep rupture life compared to the as-built and SHT-treated states **[27,28]**.

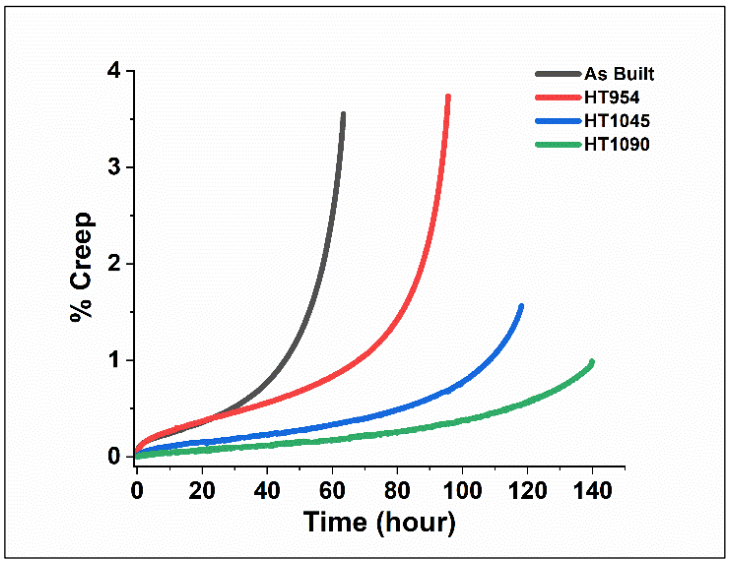

Figure 4.14. Creep curves of IN 718 at 650°C & 689 MPa

Tablo 4.8. Creep life and % creep of 718

Creep Test	% Creep	Rupture Time (H:M)
As Built	3,56	63:40
SHT	3,74	95:61
HT1045	1,57	118:15
HT1090	0,99	139:81

Strain Rate ($\dot{\varepsilon}$)

The creep rates observed in the as-built and SHT conditions are relatively high. In contrast, the creep rates of HT1045 and HT1090 are significantly lower and are also quite similar to each other.

Creep rate refers to the time-dependent plastic deformation of a material under constant stress at elevated temperatures. Creep is the gradual deformation or elongation that typically occurs in materials subjected to prolonged loading under high-temperature conditions.

The implications of a high or low creep rate are as follows:

- A high creep rate signifies that the material deforms more rapidly under a given load, indicating faster degradation and reduced mechanical integrity over time. This suggests that the material will experience fatigue and failure sooner when exposed to long-term loading conditions.

- A low creep rate, on the other hand, indicates that the material deforms more slowly, thereby enhancing its resistance to long-term stress and extending its operational life under high-temperature environments.

  Materials with low creep rates are therefore more desirable for engineering applications requiring sustained performance at elevated temperatures, as they exhibit greater durability and resistance to deformation over time.

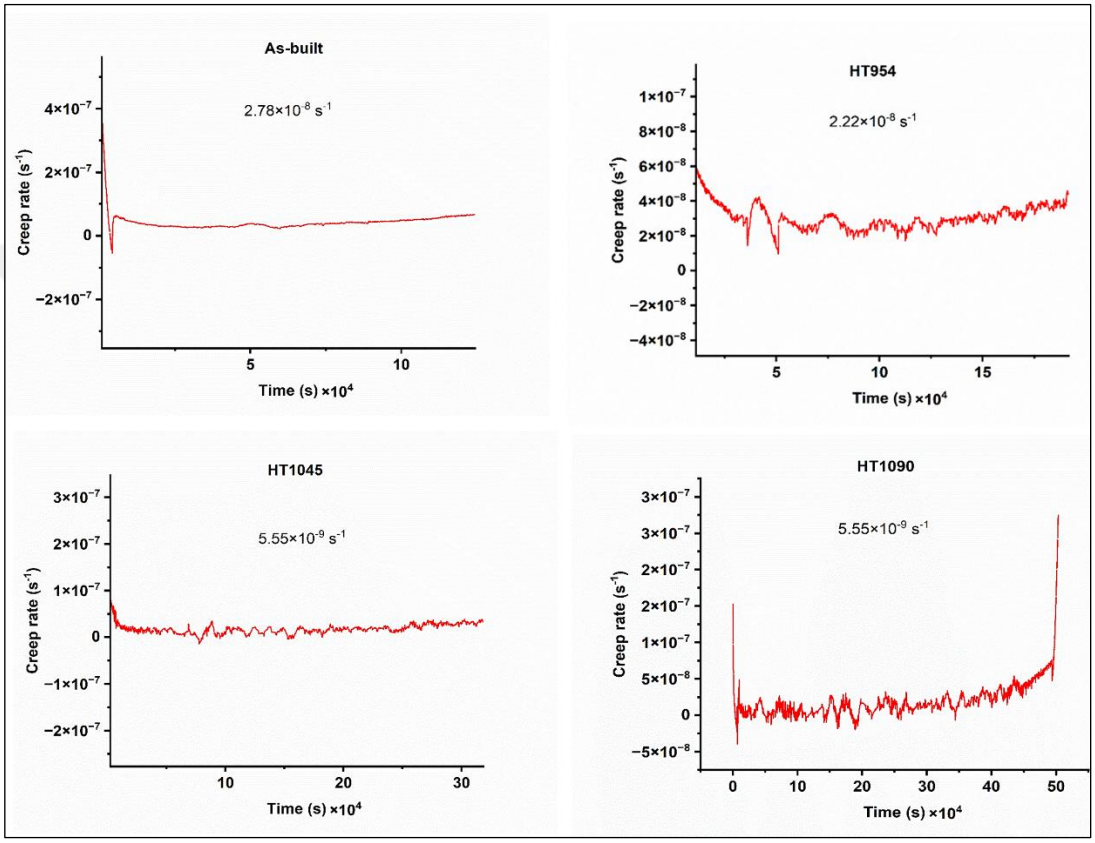

Figure 4.15. Creep rates of creep tests

5. CONCLUSION

The influence of post-processing heat treatments on the microstructure and mechanical properties of Inconel 718 alloys produced via selective laser melting (SLM) was evaluated. The following conclusions were drawn from the results:

1- As anticipated, the microstructures of Inconel 718 alloys fabricated by SLM exhibited significant differences from cast and wrought counterparts. In the lateral observation direction, a typical melt pool morphology featuring arc-shaped patterns was observed. Moreover, laser beam scanning traces were visible in the axial observation direction.

2- Melt pool structure displayed a refined cellular/columnar pattern, distinguished by irregularly shaped Laves phases located in the interdendritic areas. Moreover, the re-melting of earlier solidified layers caused the formation of overlapping regions along both the lateral and axial dimensions.

3- The SHT heat treatment proved inadequate for dispersing the Laves phases. SEM images also revealed a significant presence of delta phases, which are brittle in nature. Both Laves and delta phases were predominantly located at grain boundaries.

4- Following heat treatments under HT1045 and HT1090 conditions, the arc-shaped microstructural features were replaced by equiaxed grains. The microstructure of the heat-treated alloys featured a stable γ matrix, strengthened by coherent γ" or γ' phase particles, along with other secondary phases. Because of the low solubility of large Nb and Mo atoms in the matrix, significant amounts of undissolved Laves phases were observed.

REFERENCES

[1] S. Özer, "Effect Of Post-Processing Heat Treatment On The Mechanical Properties Of Inconel 718 Fabricated By Selective Laser Melting A Thesis Submitted To The Graduate School Of Natural And Applied Sciences Of Middle East Technical Unıversity," 2020. Accessed: Dec. 11, 2024. [Online]. Available: https://etd.lib.metu.edu.tr/upload/12625258/index.pdf

[2] Razavykia, A., Brusa, E., Delprete, C., & Yavari, R. (2020). An overview of additive manufacturing technologies—a review to technical synthesis in numerical study of selective laser melting. Materials, 13(17), 3895.

[3] Bradley, E.F., 1979, Source Book on Materials for Elevated-Temperature Applications, American Society for Metals, Metal Park, OH. 29

[4] B. Geddes, H. Leon, and X. Huang. (2010). Superalloys: Alloying and Performance. ASM International.

[5] J. B. Wahl and K. Harris. (2011). Advanced Ni base superalloys for small gas turbines. Canadian Metallurgical Quarterly, 50(3), 207-214.

[6] Smallman, R.E., Bishop, R.J., (2009), Modern Physical Metallurgy and Materials Engineering. Butterworth-Heinemann, Reed Educational and Professional Publishing Ltd.

[7] Çay, V., Ozan, S., (2005), Süperalaşımlar ve Uygulama Alanları, Doğu Anadolu Bölgesi Araştırmaları. p. 178-188.

[8] Bahadır, B., (2010), Süperalaşımların Açık ve Kontrollü atmosferde Dökümü. Yüksek Lisans Tezi, YTÜ.

[9] B. Geddes, H. Leon, and X. Huang. (2010). Superalloys: Alloying and Performance. ASM International.

[10] J. R. Davis. (2001). ASM specialty handbook: nickel, cobalt, and their alloys. ASM International.

[11] E.O. Ezugwu, Improvements in the machining of aero-engine alloys using self-propelled rotary tooling technique, J Mater Process Technol. 185 (2007) 60–71. https://doi.org/10.1016/j.jmatprotec.2006.03.112.

[12] D. Dye, O. Hunziker, S.M. Roberts, R.C. Reed, Modeling of the Mechanical Effects Induced by the Tungsten Inert-Gas Welding of the IN718 Superalloy, n.d.

[13] G. Aggen, F.W. Akstens, C. Michael, A. Adjelian, A. Rubeli, L.H.S. Avery Consultant, P. Babu, A.M. Bayer, T. Vasco, F. Bello, S.P. Bhat, M. Blair, B. Boardman, K.W. Boehm, N. Steel, F.W. Boulger, G.K. Bouse, J.L. Bowles, J.D. Boyd, B.L. Bramfitt, R.W. Bratt, W.D. Brentnall, ASM Handbook, Volume 1, Properties and

Selection: Irons, Steels, and High Performance Alloys Section: Publication Information and Contributors Publication Information and Contributors Authors and Reviewers, 2005.

[14] J. Smialek, Protective alumina scales View project High temperature corrosion View project, n.d. https://www.researchgate.net/publication/283993132.

[15] A. Chamanfar, L. Sarrat, M. Jahazi, M. Asadi, A. Weck, A.K. Koul, Microstructural characteristics of forged and heat treated Inconel-718 disks, Mater Des. 52 (2013) 791–800. https://doi.org/10.1016/j.matdes.2013.06.004.

[16] C.M. Kuo, Y.T. Yang, H.Y. Bor, C.N. Wei, C.C. Tai, Aging effects on the microstructure and creep behavior of Inconel 718 superalloy, Materials Science and Engineering A. 510–511 (2009) 289–294. https://doi.org/10.1016/j.msea.2008.04.097.

[17] Li, X., Shi, J. J., Wang, C. H., Cao, G. H., Russell, A. M., Zhou, Z. J., ... & Chen, G. F. (2018). Effect of heat treatment on microstructure evolution of Inconel 718 alloy fabricated by selective laser melting. Journal of Alloys and Compounds, 764, 639-649.

[18] Özer, S. (2020). Effect of post-processing heat treatment on the mechanical properties of inconel 718 fabricated by selective laser melting (Master's thesis, Middle East Technical University).

[19] Pan, H., Dahmen, T., Bayat, M., Lin, K., & Zhang, X. (2022). Independent effects of laser power and scanning speed on IN718's precipitation and mechanical properties produced by LBPF plus heat treatment. Materials Science and Engineering: A, 849, 143530.

[20] Bassini, E., Marchese, G., & Aversa, A. (2021). Tailoring of the microstructure of laser powder bed fused Inconel 718 using solution annealing and aging treatments. Metals, 11(6), 921.

[21] Calandri, M., Yin, S., Aldwell, B., Calignano, F., Lupoi, R., & Ugues, D. (2019). Texture and microstructural features at different length scales in Inconel 718 produced by selective laser melting. Materials, 12(8), 1293.

[22] Li, X., Shi, J. J., Wang, C. H., Cao, G. H., Russell, A. M., Zhou, Z. J., ... & Chen, G. F. (2018). Effect of heat treatment on microstructure evolution of Inconel 718 alloy fabricated by selective laser melting. Journal of Alloys and Compounds, 764, 639-649.

[23] Xu, J., Ma, T., Peng, R. L., & Hosseini, S. (2021). Effect of post-processes on the microstructure and mechanical properties of laser powder bed fused IN718 superalloy. Additive Manufacturing, 48, 102416.

[24] Zhang, D., Niu, W., Cao, X., & Liu, Z. (2015). Effect of standard heat treatment on the microstructure and mechanical properties of selective laser melting manufactured Inconel 718 superalloy. Materials Science and Engineering: A, 644, 32-40.

[25] Diepold, B., Vorlaufer, N., Neumeier, S., Gartner, T., & Göken, M. (2020). Optimization of the heat treatment of additively manufactured Ni-base superalloy IN718. International Journal of Minerals, Metallurgy and Materials, 27, 640-648.

[26] Zhang, S., Lin, X., Wang, L., Yu, X., Yang, H., Lei, L., & Huang, W. (2021). Influence of grain inhomogeneity and precipitates on the stress rupture properties of Inconel 718 superalloy fabricated by selective laser melting. Materials Science and Engineering: A, 803, 140702.

[27] Kuo, Y. L., Nagahari, T., & Kakehi, K. (2018). The effect of post-processes on the microstructure and creep properties of alloy718 built up by selective laser melting. Materials, 11(6), 996.

[28] Gao, Y., Zhang, D., Cao, M., Chen, R., Feng, Z., Poprawe, R., ... & Ziegler, S. (2019). Effect of δ phase on high temperature mechanical performances of Inconel 718 fabricated with SLM process. Materials Science and Engineering: A, 767, 138327.

[29] Shi, J. J., Zhou, S. A., Chen, H. H., Cao, G. H., Russell, A. M., Zhou, Z. J., ... & Chen, G. F. (2021). Microstructure and creep anisotropy of Inconel 718 alloy processed by selective laser melting. Materials Science and Engineering: A, 805, 140583.

BIOGRAPHY

I completed my high school education at Öğretmen Mukadder Akaydın Anatolian High School in Çorum. In 2015, I started my undergraduate studies in the Department of Materials Science and Engineering at Gebze Technical University, and I graduated in January 2021. In 2021, I began my master's degree in the same department at Gebze Technical University. During my master's studies, I worked as a scholarship member in the Metallic Materials Technologies Research Group at TÜBİTAK MAM. I participated in the "3219504 UP26-SAYEM Eklemeli İmalata Yönelik Yerli ve Özgün Tasarım, Malzeme, Üretim ve Tezgah Teknolojilerinin Geliştirilmesi Platformu" project.

PUBLICATION AND PRESENTATIONS FROM THE THESIS

Canbolat M., Tamsü-Selli N., Aydın H., "Effect of Post Processing Heat Treatments on the Microstructure and Creep Properties of Additively Manufactured IN718", 22nd International Metallurgy and Materials Congress, 19-21 September 2024, İstanbul/Türkiye. (Oral Presentation)

Canbolat M., Tamsü-Selli N., Aydın H., "Microstructural and High Temperature Mechanical Behaviour As-Built and Heat Treated INCONEL 718", Gebze Teknik Üniversitesi 8. Lisansüstü Araştırmaları Sempozyumu, 30-31 May 2024, Kocaeli/Türkiye. (Oral Presentation)